Speed Regulated Continuous DTC Induction Motor Drive in Field Weakening

Petar MATIĆ[1], Slobodan N. VUKOSAVIĆ[2]
[1]*Faculty of Electrical Engineering, University in Banjaluka, Republic of Srpska, BiH*
[2]*Faculty of Electrical Engineering, University in Belgrade, Serbia*
petar.matic@etfbl.net

***Abstract*—The paper describes sensorless speed controlled continuous Direct Torque Control (DTC) Induction Motor (IM) drive in the field weakening regime. Drive comprises an inner torque loop and an outer speed loop. Torque control is based on Proportional - Integral (PI) controller with adaptive Gain Scheduling (GS) parameters. The GS PI control provides full DC link voltage utilization and a robust disturbance rejection along with a fast torque response. Outer speed loop has a PI regulator with the gains selected so as to obtain a fast and strictly aperiodic response. Proposed drive fully utilizes the available DC bus voltage. The paper comprises analytical considerations, simulation results, and detailed description of the implementation steps. Experimental verification of the proposed solution is conducted on a fixed point Digital Signal Processor (DSP) platform.**

***Index Terms*—adaptive control, digital signal processors, induction motor drives, torque control, velocity control**

I. INTRODUCTION

The term DTC usually refers to a specific control scheme based on the torque and flux hysteresis comparator without the inner current loop [1]. The method controls the motor by electing one discrete voltage vector and applying it over the whole switching period [2] - [4]. In this paper, the control scheme is proposed wherein the sequence of three voltage vectors is altered within each switching period. This contributes to a smooth change in the average voltage and a lower current ripple. The voltage generation is based on continuous stator voltage vectors obtained by Space Vector Modulation technique with the constant switching frequency [5] - [8].

In IM drives the flux is kept constant below the rated speed and decreased as the drive enters the high speed region [9]. Flux and torque producing components of induction motor in the field weakening regime are coupled due to the voltage limit [10], [11]. The only independent control variable in this regime is the angle of the stator voltage [12]. The concept of this paper is to propose sensorless speed controlled drive which uses all of the available DC bus voltage. In presented approach, retention of certain voltage margins is not necessary due to the torque being controlled by the voltage angle, and the approach is applicable both in linear regime and in overmodulation.

It is shown in [12] that with the angle and the gain–scheduling both torque and flux can be controlled without an explicit flux reference or a preprogrammed trajectory and without the inner current loop. Flux optimization is intrinsically accomplished by the closed loop operation of the proposed structure.

In numerous applications of servo drives, overshooting the speed setpoint is not acceptable [13], [14]. The overshoot may result in bringing the mechanical load and its vital parts, such as the tools, into a condition where they may eventually break. Therefore, in a number of applications, it is desirable to have the speed step response without an overshoot and the driving torque transient with no oscillations. Speed regulator proposed in the paper enables aperiodic speed response, avoids speed overshoots and oscillations even in case of large input disturbances [13]. Stability of the proposed drive in field weakening is preserved by limiting output of the speed regulator to the break-down torque in an original manner.

The paper is organized as follows. In Section IIa nonlinear state-space model of IM is developed. The model is based on the assumption that the drive operating in the field weakening mode makes full utilization of the DC bus voltage [12]. In order to get an insight into torque dynamics, a small signal model is developed (Section IIb). Instead of deriving the accurate transfer function of the small signal model, a simplified nominal linearized transfer function is adopted (Section IIc). Proposed DTC structure is described in Section III. Torque and speed regulators are explained in detail in sections IIIa and IIIb, respectively, while the estimator is explained in Section IIIc. Verification of the proposed solution by simulation and experiment is given in Sections IV and V. Results are discussed and remarks are given on controllers' performance. Conclusion is given in Section VI.

II. MATHEMATICAL BACKGROUND

A. *Nonlinear Model of Induction Motor*

Assuming synchronous frequency ω_e as the control variable, motor torque t_e as the output variable, and the reference frame aligned with stator voltage:

$$u_{sd} = U\ ,\ u_{sq} = 0\ , \tag{1}$$

nonlinear model in the space of normalized (in per-unit [p.u]) stator and rotor fluxes:

$$\boldsymbol{\Psi} = \begin{bmatrix} \Psi_d & \Psi_q & \Psi_D & \Psi_Q \end{bmatrix}^T , \tag{2}$$

is given as follows:

This work was supported by Ministry of Science and Technology of Republika Srpska.

Digital Object Identifier 10.4316/AECE.2011.01016

$$\frac{\mathrm{d}\boldsymbol{\Psi}}{\mathrm{d}t}=\mathbf{A}(\omega_e,s)\boldsymbol{\Psi}+\omega_b\begin{bmatrix}U & 0 & 0 & 0\end{bmatrix}^T, \tag{3}$$

$$\mathbf{A}(\omega_e,s)=\omega_b\begin{bmatrix}1/T_s^{'} & \omega_e & k_r/T_s^{'} & 0\\ -\omega_e & -1/T_s^{'} & 0 & k_r/T_s^{'}\\ k_s/T_r^{'} & 0 & -1/T_r^{'} & s\omega_e\\ 0 & k_s/T_r^{'} & -s\omega_e & -1/T_r^{'}\end{bmatrix}, \tag{4}$$

$$t_e=\frac{1}{\sigma l_s}\left(\Psi_D\Psi_q-\Psi_Q\Psi_d\right). \tag{5}$$

$$T_m\frac{\mathrm{d}\omega}{\mathrm{d}t}=t_e-t_L. \tag{6}$$

In the model (2) – (6), u_d, u_q, Ψ_d, Ψ_q, Ψ_D, Ψ_Q are voltage and flux components, s is relative slip, ω_b is base speed, $k_s=M/L_s$ and $k_r=M/L_r$ are stator and rotor coupling coefficients, $T_s^{'}=\omega_b\sigma L_r/R_s$ and $T_r^{'}=\omega_b\sigma L_r/R_r$ are stator and rotor transient time constants in [p.u], R_s and R_r are stator and rotor resistance, L_s and L_r are stator and rotor self–inductances, M is mutual inductance, $\sigma=1-M^2/L_sL_r$ is leakage coefficient, l_s is stator inductance in [p.u], T_m is mechanical time constant and t_L is load torque in [p.u].

B. *Small Signal Model*

For the given operation regime $(\omega_e,s)=\left(\omega_e^0,s^0\right)$, nonlinear model (2) – (4) gives steady-state vector of fluxes:

$$\boldsymbol{\Psi}^0\left(\omega_e^0,s^0\right)=-\mathbf{A}^{-1}\left(\omega_e^0,s^0\right)\omega_b\begin{bmatrix}U & 0 & 0 & 0\end{bmatrix}^T \tag{7}$$

and linearized model in the form:

$$\dot{\mathbf{x}}=\mathbf{A}\left(\omega_e^0,s^0\right)\mathbf{x}+\mathbf{B}\left(\omega_e^0,s^0\right)u,\ y=\mathbf{C}\left(\omega_e^0,s^0\right)\mathbf{x}, \tag{8}$$

where: $\mathbf{A}\left(\omega_e^0,s^0\right)$ is given in (4) for $(\omega_e,s)=\left(\omega_e^0,s^0\right)$, and:

$$\mathbf{B}\left(\omega_e^0,s^0\right)=\omega_b\begin{bmatrix}0 & 1 & 0 & 0\\ -1 & 0 & 0 & 0\\ 0 & 0 & 0 & 1\\ 0 & 0 & -1 & 0\end{bmatrix}\boldsymbol{\Psi}^0\left(\omega_e^0,s^0\right), \tag{9}$$

$$\mathbf{C}\left(\omega_e^0,s^0\right)=\frac{k_r}{\sigma l_s}\boldsymbol{\Psi}^{0T}\left(\omega_e^0,s^0\right)\begin{bmatrix}0 & 0 & 0 & -1\\ 0 & 0 & 1 & 0\\ 0 & 1 & 0 & 0\\ -1 & 0 & 0 & 0\end{bmatrix}. \tag{10}$$

C. *Nominal Linear Model*

Since analytic solution for the transfer function out of state-space representation (8)–(10) is rather complicated, approximated transfer function (torque-synchronous speed) is adopted in the form of static gain plus the complex-conjugate pairs of stator-related and rotor-related poles, while finite zeros have been neglected [12]:

$$G_{App}(p)=\frac{G_{0App}}{\left(1+\frac{2\xi_s}{\omega_{ns}}p+\frac{1}{\omega_{ns}^2}p^2\right)\left(1+\frac{2\xi_r}{\omega_{nr}}p+\frac{1}{\omega_{nr}^2}p^2\right)}, \tag{11}$$

where stator and rotor damping ratios (ξ_s, ξ_r) and natural frequencies (ω_{ns}, ω_{nr}) are:

$$\xi_s=1/\sqrt{\left(1+\omega_e^2T_s^{'2}\right)}, \tag{12}$$

$$\xi_r=1/\sqrt{\left(1+s^2\omega_e^2T_r^{'2}\right)}, \tag{13}$$

$$\omega_{ns}=\omega_b\sqrt{\frac{1}{T_s^{'2}}+\omega_e^2}, \tag{14}$$

$$\omega_{nr}=\omega_b\sqrt{\frac{1}{T_r^{'2}}+s^2\omega_e^2}. \tag{15}$$

Complex operator is denoted by p. Maximal value of static gain appears under no load operation [12] and equals to:

$$G_{0App}=\frac{k_sk_rT_r^{'}U^2}{\sigma l_s\omega_e^2}. \tag{16}$$

III. Proposed Control Scheme

The proposed control scheme consists of outer speed and inner torque loop as shown in Fig. 1. The input to the control algorithm is the speed reference, which is fed to the speed regulator. Output of the speed regulator is torque reference, which is limited to the break-down value in order to preserve system stability. Estimated torque is subtracted from the torque reference and resulting torque error signal is fed to the torque controller block. Torque controller is gain - scheduled proportional-integral controller with saturation. Output of the regulator is machine slip which is limited to the motor break-down slip as $s\le\pm1/T_r^{'}$. Saturation is adjusted to prevent windup of the torque control loop. The output of the torque controller is the slip angular frequency command, which represents an increment to the estimated rotor speed. As it can be seen in Fig. 1, torque PI regulator gain is operating point sensitive, i.e. gains are scheduled by DC bus voltage and synchronous speed. Gain scheduling mechanism adopts torque controller to obtain projected response for all working points by using maximal voltage available. Reference synchronous speed is obtained by adding reference slip with the estimated speed ω_m^E. Speed command is integrated and the voltage angle command ϑ is calculated. This angle command is used to generate stationary-frame voltage commands:

$$U_\alpha=U\cos\vartheta, \tag{18}$$

$$U_\beta=U\sin\vartheta. \tag{19}$$

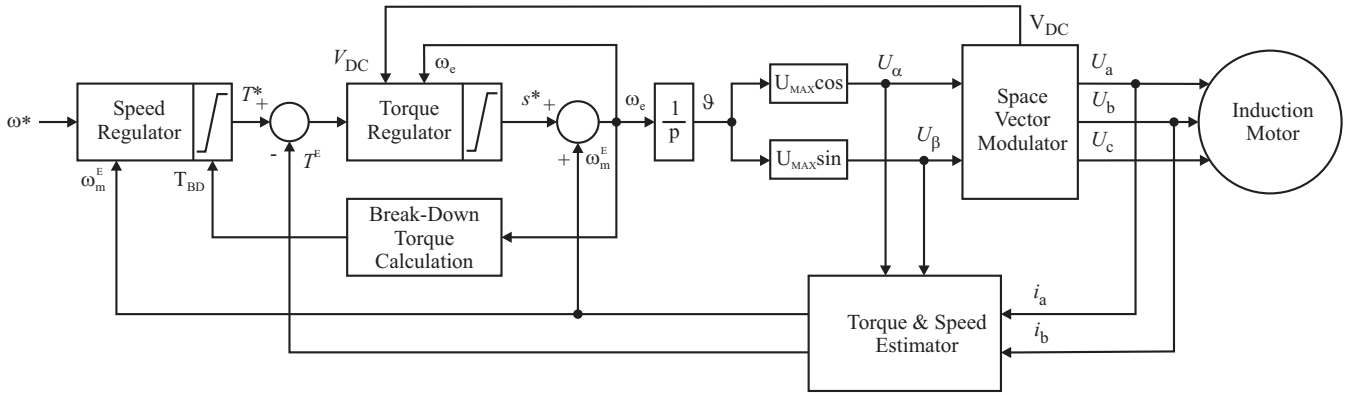

Figure 1. Proposed DTC Speed Regulated Control Scheme

Reference voltages are fed to the Space Vector Modulator to generate machine voltages U_a, U_b and U_c. Two line currents, i_a and i_b are measured. Estimated values of motor torque and rotor speed are denoted with superscript "E". A simple open loop flux estimator based on stationary frame stator voltage equations in normalized form can be used in field weakening [10]-[12].

In the following subsections, structure of torque and speed control loops as well as parameterization of the regulators will be explained.

A. *Torque Regulator*

The core of the DTC speed regulated drive is torque regulator by which the output torque t_e tracks reference input torque T_e^*. It is desirable that the response of the output torque to step input has rising edge as fast as possible and lowest transport delay. Finite response rate of electrical subsystem influences dynamics of outer speed-controlled loop.

As the natural frequency of the stator poles (14) significantly exceeds the natural frequency of the rotor poles (15), the dynamic torque response in the field weakening regime is determined predominantly by the rotor dynamics. Static gain (16) depends both on synchronous frequency and slip and has its maximal value when slip is equal to zero [12]. The torque regulator is parameterized in the form:

$$\frac{T^*(p)}{s^*(p)} = K_{PI}(p) = K_C\left(\frac{1}{\omega_C} + \frac{1}{p}\right), \tag{17}$$

Where ω_C is desired closed-loop bandwidth and K_C is the regulator gain needed to achieve it. Closed-loop bandwidth ω_C is selected as a half rotor natural frequency for unloaded motor, as this is considered to be the worst case (with the lowest phase margin). Adequate tuning of PI regulator parameters is:

$$\omega_C = \omega_b / 2T_r^{'}, \tag{18}$$

$$K_C = \frac{\omega_C}{G_{0AppMAX}} = \frac{\omega_b \sigma l_s}{2k_s k_r T_r^{'2} U^2}\omega_e^2. \tag{19}$$

Gain of PI regulator (17) depends on both synchronous speed and supply voltage, i.e. gain scheduling mechanism is introduced.

B. *Speed Regulator*

In many applications it is required that steady state speed error is equal to zero at constant reference input with strictly aperiodic response and short settling time. Since the inner torque loop has much higher bandwidth than outer speed loop (defined by the speed loop sampling time $T_{s\omega}$) torque regulation subsystem can be modeled as continuous transfer function. The delay of torque response should be taken into account during the synthesis of speed loop and choosing the parameters of speed regulator. It can be approximated by the first-order time delay as:

$$\frac{T^*(p)}{t_e(p)} = \frac{K_m}{1 + p\tau_e}, \tag{20}$$

where τ_e is dominant time constant of electrical subsystem, and K_m is torque gain. If the adopted time constant has higher value than actual, than the speed response would be unnecessarily slow. On the contrary speed response would have overshoots due to increased bandwidth for lower estimated values of time constant. To avoid the overshoot, the speed controller design has to provide a closed-loop system transfer function without zeros. The solution to the problem is the relocation of the proportional gain [13], [14] as shown in Fig. 2. By moving the proportional gain into the feedback path, a finite zero which should appear in closed-loop transfer function is eliminated. Since the only integral gain is located in the path of error signal, the sudden jump of reference torque T^* is avoided when speed setpoint is changed.

The maximum torque available on the motor shaft in field weakening is limited by the characteristics of the power converter and the motor itself. In field weakening, motor current is limited due to power switches capabilities while the torque value is limited to the break – down torque value. Since the break-down torque limit is usually stronger than current limit in field weakening [9]-[12], torque limit is considered only. Value of the break-down torque is given in (21) assuming that rotor resistance can be neglected in field weakening [6]. Since the break down torque (21) depends on voltage and synchronous speed, the limit T_{BD} shown in Fig. 2 should be adopted dynamically.

$$T_{BD} = \frac{1}{2}\frac{1-\sigma}{\sigma l_s}\frac{U^2}{\omega_e^2}. \tag{21}$$

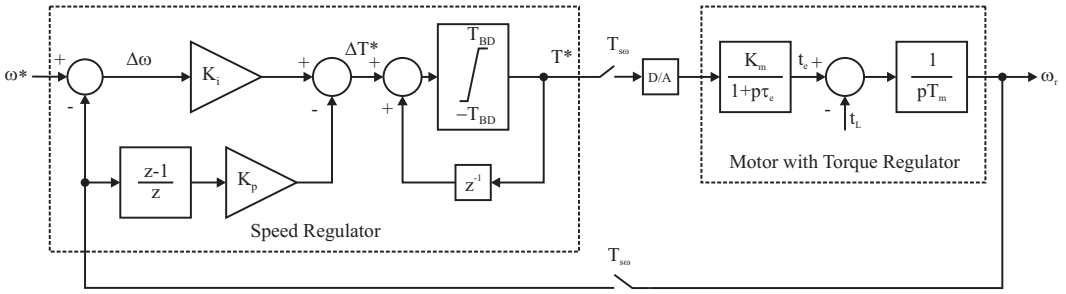

Figure 2. Speed Control Loop Structure

When speed disturbance is such that the torque requirement exceeds the limit, system operates in nonlinear mode leading to the wind-up of speed regulator. To prevent wind-up, an incremental form of the PI speed controller is used [14] based on the sum of proportional and integral actions. To calculate increment in the proportional action, $K_P\left(\omega_{r(k+1)}-\omega_{r(k)}\right)$, delay block for speed is introduced, while increment of the integral action is obtained by multiplying the gain K_I with the new sample of the speed error $\Delta\omega=\omega^*-\omega_{r(k)}$. The increments of the proportional and integral action are summed, and new torque increment $\Delta T^*_{(k+1)}$ is obtained. This increment is added to the most recent value of the torque reference, obtained at the previous sampling instant from z^{-1} operator block. Since the torque reference T^* is obtained at the output of the torque limiter, it is ensured that the actual torque reference never exceeds the limit T_{BD}.

In linear mode, when driving torque stays within the limits, the torque limiter acts as the unity gain block, thus enabling accumulating the torque reference in the conjunction with z^{-1} block, constituting discrete-time integrator. In non-linear mode, the torque limiter prevents the integrator wind-up and limits torque reference T^* to the break-down torque T_{BD}.

The structure of speed regulator in Fig. 2 makes possible realization of strictly aperiodical response, without speed overshoots, by choosing optimal values of parameters K_P and K_I. It is shown [13], [14] that optimal tuning of control parameters is reduced to the determination of the minimum of the ratio K_P/K_I under the condition that all zeros of the characteristic polynomial of closed-loop transfer function lay on the positive part of the real axis inside unit circle with center at the origin of the z plane.

Optimal values of the speed PI regulator gains are found to be:

$$K_P=\frac{\sigma^3-\beta}{(1-\beta)C}, \tag{22}$$

$$K_I=\frac{3\sigma^2-1-2\beta}{(1-\beta)C}, \tag{23}$$

where coefficients in (22) and (23) are from [13] $\beta=\exp(-T_{s\omega}/\tau_e)$, $\sigma=\sqrt[3]{4+4\beta}-1$, $C=(K_mT_{s\omega})/(2T_m)$ respectively.

C. Torque and Speed Estimator

In field weakening, back electromotive forces are relatively large [10]-[12], so a simple open loop flux estimator based on stationary frame stator space vector equations can be used. Estimated values are denoted with the superscript "E". Stator flux vector is given as follows:

$$\boldsymbol{\Psi}^E_{\alpha\beta}=\omega_b\int\left(\mathbf{U}_{\alpha\beta}-r_s\mathbf{i}_{\alpha\beta}\right)dt. \tag{24}$$

Stator currents in stationary reference frame are calculated from measured currents. Estimated motor torque is found from stator flux and conjugate stator current as:

$$T^E=-\mathrm{Im}\left\{\boldsymbol{\Psi}^E_{\alpha\beta}\cdot\mathbf{i}^*_{\alpha\beta}\right\}, \tag{25}$$

and estimated rotor flux space vector is:

$$\boldsymbol{\Psi}^E_{\alpha\beta r}=\frac{1}{k_r}\left(\boldsymbol{\Psi}^E_{\alpha\beta}-\sigma l_s\mathbf{i}_{\alpha\beta}\right). \tag{26}$$

Motor slip is calculated from estimated torque and estimated rotor flux space vector modulus as:

$$s^E=\left(r_rT^E\right)/\left|\boldsymbol{\Psi}^E_{\alpha\beta r}\right|^2. \tag{27}$$

Rotor speed is calculated from estimated synchronous speed which is obtained from rotor flux angle:

$$\omega^E_e=\frac{\mathrm{d}}{\mathrm{d}t}\left(\arg\boldsymbol{\Psi}^E_{\alpha\beta r}\right), \tag{28}$$

by subtracting estimated slip as:

$$\omega^E_m=\omega^E_e-s^E. \tag{29}$$

In practical realization, instead of pure integration (24), the low pass filter should be used to avoid integrator drift.

IV. Simulation Results

Initial verification of the proposed approach is done by series of computer simulations. Control scheme depicted in Fig. 1 with neglible torque response delay time (20) is implemented. Simulation results are given in Figs. 3-7.

Closed-loop responses when speed reference changes from 1 to 2 p.u in form of steps is shown in Figs. 3-5. As seen from Fig. 3, speed response is strictly aperiodic, while the rotor flux decreases as speed increases. Stator current and motor torque are shown in Fig. 4. It can be seen that torque response is without oscillations and the torque is limited to the break-down value when speed reference suddenly changes. The synchronous speed and slip speed are shown in Fig. 5. It can be seen that for larger values of speed, slip speed increases since the rotor flux decreases.

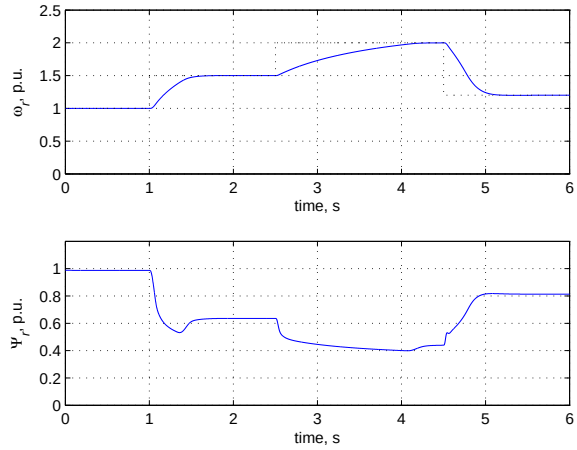

Figure 3. Shaft Speed and Rotor Flux

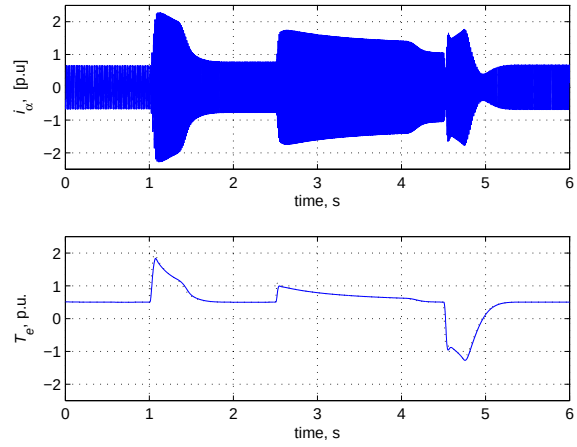

Figure 4. Stator Current and Motor Torque

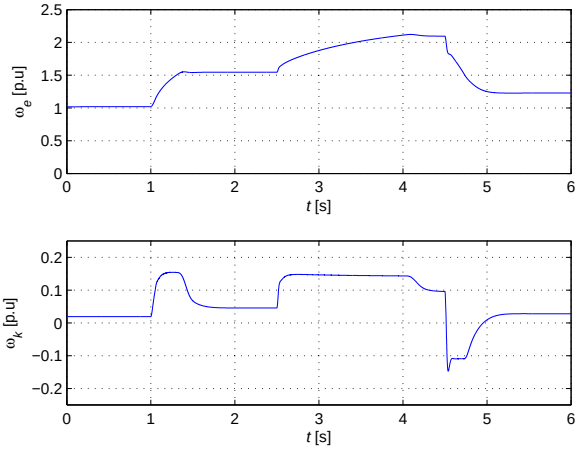

Figure 5. Synchronous and Slip Speed

Rotor flux, shown in Fig. 3 decreases as speed increases. Proposed DTC structure enables rotor flux regulation without outer flux reference trajectory. In the simulation, the motor was loaded with the constant load torque equal to 0.5 p.u, as it can be seen in Fig. 4 and Fig. 5.

Simulation results when unloaded machine accelerates from 2 to 3.5 p.u. are shown in Fig. 6 and Fig. 7. Even the input disturbance is very large, speed response is fast and strictly aperiodic as seen in Fig. 6. Since the output of the speed regulator is limited to the break-down torque, motor torque decreases as speed increases, Fig. 7.

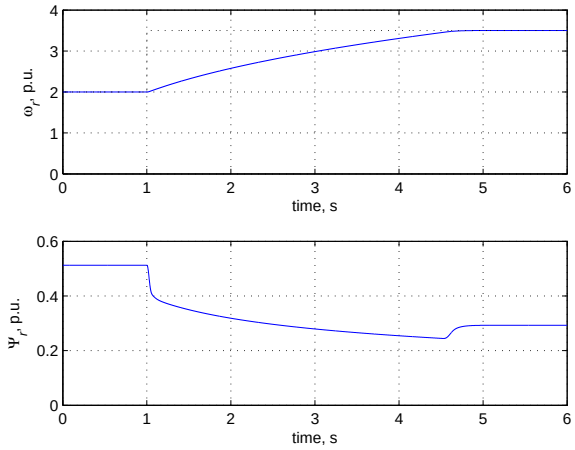

Figure 6. Shaft Speed and Rotor Flux

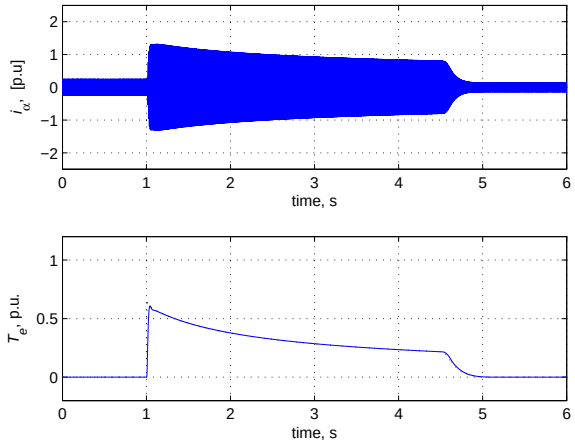

Figure 7. Stator Current and Motor Torque

V. EXPERIMENTAL VERIFICATION

Experimental verification is done on a test setup with two mechanically coupled induction machines powered by two inverters with paralleled DC busses. The control algorithm is implemented on fixed point processor DSP board.

The inner torque control loop without speed regulator in order to obtain the delay time and gain of torque loop (20) is tested first. Torque reference was in form of rectangular pulses to simulate a step change in load (Fig. 8). The shaft speed was kept constant on 2.5 p.u. by load machine (Fig 9). From Fig. 8, parameters of (20) are $\tau_e = 0.05\text{s}$ and $K_m = 1$.

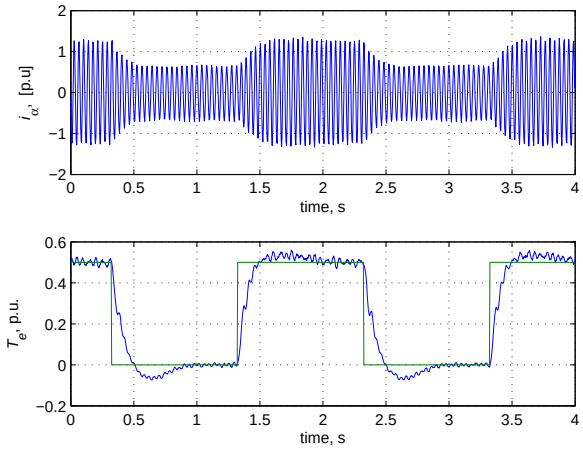

Figure 8. Stator Current and Motor Torque

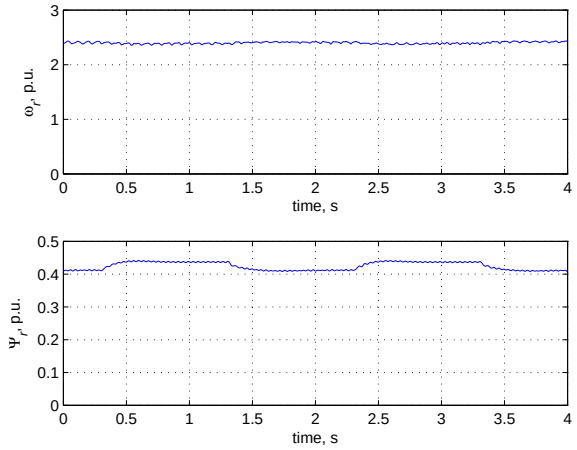

Figure 9. Shaft Speed and Rotor Flux

Closed loop performances of the speed regulated DTC drive are shown through Figs. 10-11. All references are plotted with dashed lines. The speed reference was changed from 2 p.u. to 3.5. p.u. as shown in Fig. 10. Stator current and motor torque are shown in Fig. 11.

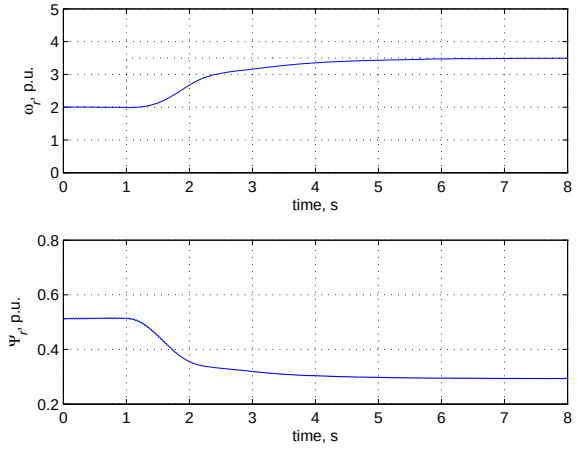

Figure 10. Shaft Speed and Rotor Flux

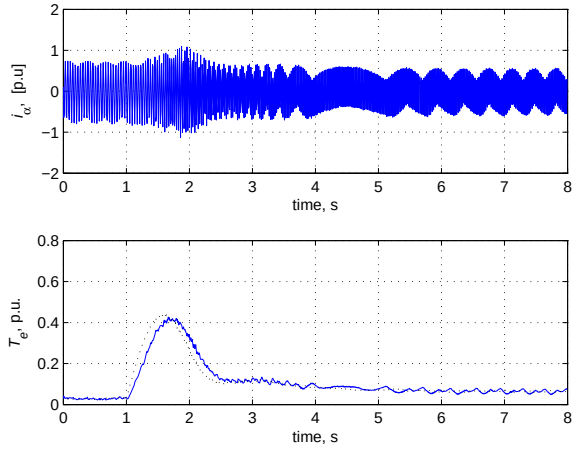

Figure 11. Stator Current and Motor Torque

The trace corresponding to the shaft speed in Fig. 10 is strictly aperiodic and does not overshoot the set point. While the speed approaches the set point, the driving torque does not change its sign and remains strictly positive. The rotor flux decreases without oscillations as speed increases. Since the friction losses increase as speed increases, the steady state torque is larger when the speed is larger, as it can be seen in Fig. 11.

VI. CONCLUSION

The proposed DTC IM drive in field weakening enables fast and accurate speed regulation. Drive does not require flux reference calculation, nor the current regulator. Best possible DC bus voltage utilization in field weakening is obtained by only regulating the voltage angle. Torque regulator with gain scheduling provides well damped torque response. Proposed speed regulator enables aperiodic speed response, avoids speed overshoots and oscillations even in case of large disturbance input signals. Computer simulation and experiment prove excellent performances of the drive.

VII. APPENDIX

Parameters of motor used in simulation and experiment are 750W, 380V, 50Hz, 1450rpm, $R_s = 10.5\Omega$, $R_r = 11\Omega$, $M = 0.557\text{H}$, $L_s = 0.579\text{H}$, $L_r = 0.579\text{H}$.

REFERENCES

[1] D. Casadei, F. Profumo, G. Serra, A. Tani, "FOC and DTC: Two Viable Schemes for Induction Motor Torque Control", IEEE Transactions on Power Electronics, Vol. 17, No.5, pp. 779-787, September 2002.

[2] Z. Sorchini, P. Krein, "Formal Derivation of Direct Torque Control for Induction Machines", IEEE Transactions on Power Electronics, Vol. 21, No.5, pp. 1428-1436, September 2006.

[3] Mohamed Bounadja, Ahmed W. Belarbi, Bachir Belmadani, "A High Performance Space Vector Modulation Direct Torque Controlled Induction Machine Drive based on Stator Flux Orientation Technique", Advances in Electrical and Computer Engineering, Volume 9, Number 2, pp. 28-33, 2009.

[4] Pavel Brandstetter, Petr Chlebis, Petr Palacky, "Direct Torque Control of Induction Motor with Direct Calculation of Voltage Vector", Advances in Electrical and Computer Engineering, Volume 10, Number 4, pp 17-22, 2010.

[5] D. Casadei, G. Serra, A. Tani, L. Zarri, F. Profumo, "Performance Analysis of a Speed Sensorless Induction motor Drive Based on a Constant Switching Frequency DTC Scheme", IEEE Transactions on Industry Applications, Vol. 39, No. 2, March/April 2003.

[6] P. Matić, B. Blanuša, S. N. Vukosavić, "A Novel Direct Torque and Flux Control Algorithm for the Induction Motor Drive", IEEE International Electric Machines and Drives Conference, IEMDC'03, Proceedings, Vol. 2, pp. 965-970, 1-4. June 2003.

[7] Dj. M. Stojic, S. N. Vukosavic, "A New Induction Motor Drive Based on the Flux Vector Acceleration Method", IEEE Transactions on Energy Conversion, Vol. 20, No. 1, pp.173-180, March 2005.

[8] Sergiu Ivanov, "Continuous DTC of the Induction Motor", Advances in Electrical and Computer Engineering, Volume 10, Number 4, pp. 149-154, 2010.

[9] Lennart Harnefors, Kai Pietilainen, Lars Gertmar, "Torque – Maximizing Field-Weakening Control: Design, Analysis, and Parameter Selection", IEEE Transactions on Industrial Electronics, Vol. 48, No.1, February 2001.

[10] D Casadei, G. Serra, A. Stefani, A. Tani, L. Zarii, "DTC Drives for Wide Speed Range Applications Using a Robust Flux – Weakening Algorithm", IEEE Transactions on Industrial Electronics, Vol. 54, No.5, October 2007.

[11] M. Mengoni, L. Yarri, A. Tani, G. Serra, D. Casadei, "Stator Flux Vector Control of Induction Motor Drive in the Field Weakening Region", IEEE Transactions on Power Electronics, Vol. 23, No. 2, pp. 941-949, March 2008.

[12] P. Matić, S. N. Vukosavić, A. Rakić, „Induction Motor Torque Control in Field Weakening Regime by Voltage Angle Control", 14th EPE-PEMC Conference, Ohrid, 6-8. September 2010.

[13] Milic R. Stojic, Slobodan N. Vukosavic, "Design of Microprocessor Based System for Positioning Servomechanism with Induction Motor", IEEE Transactions on Industrial Electronics, Vol. 38, No5, pp. 369-378, October 1991.

[14] S. N. Vukosavić, "Digital Control of Electric Drives", Springer, New York, 2007.